

## Nonlinear Magneto-optic Effects with Ultranarrow Widths

Dmitry Budker,<sup>1,2</sup> Valeriy Yashchuk,<sup>1,3</sup> and Max Zolotarev<sup>2</sup>

<sup>1</sup>*Department of Physics, University of California, Berkeley, California 94720-7300*

<sup>2</sup>*E. O. Lawrence Berkeley National Laboratory, Berkeley, California 94720*

<sup>3</sup>*B. P. Konstantinov Petersburg Nuclear Physics Institute, Gatchina, Russia 188350*

(Received 17 July 1998)

Several dispersionlike features in the magnetic field dependence of the nonlinear magneto-optic effect were observed in an experiment performed on rubidium atoms contained in a vapor cell with antirelaxation coating. The narrowest feature has effective resonance width  $\gamma = g\mu\Delta B_z \approx 2\pi \times 1.3$  Hz, where  $\Delta B_z \approx 2.8$   $\mu$ G is the peak-to-peak separation. The observed nontrivial dependence of the magneto-optic effect on transverse magnetic fields is discussed. The results of this work may be applied to low-field magnetometry, to parity and time reversal invariance violation experiments, etc. [S0031-9007(98)07938-1]

PACS numbers: 42.50.Gy, 07.55.Ge, 32.80.Bx, 42.65.Vh

Nonlinear (in light power) magneto-optic effects (NMOE) related to the interaction of near-resonant light with atomic vapor in the presence of a magnetic field have been the subject of a number of recent investigations reviewed in [1]. Most of the work (see, e.g., Refs. [2–8]) addresses NMOE in the case of linearly polarized light propagating along the magnetic field known as nonlinear Faraday rotation. The magnetic field dependence of this effect exhibits several dispersionlike features with widths determined by different relaxation processes. The feature reaching a maximum at several gauss is due to hole burning in the atomic velocity distribution. Its effective width  $\sim 1$ – $10$  MHz is determined by the natural width of the excited state. Significantly narrower features arise due to long-lived light-induced alignment of the atomic ground state. In this work we have observed the narrowest NMOE feature corresponding to an effective width  $\gamma = g\mu\Delta B_z \approx 2\pi \times 1.3$  Hz, where  $g$  is the Landé factor,  $\mu$  is the Bohr magneton, and  $\Delta B_z$  is the peak-to-peak separation of the feature. This is about 3 orders of magnitude narrower than the NMOE widths observed by other authors [8] and over an order of magnitude narrower than our earlier result [9].

We have studied NMOE with <sup>85</sup>Rb atoms contained in a vapor cell. The cell (diameter  $d = 10$  cm) has a high quality paraffin coating [10] in order to reduce the relaxation of the ground state polarization in wall collisions [11]. The experiments were performed on the  $D_2(2S_{1/2} \rightarrow 2P_{3/2}; \lambda = 780.2$  nm) resonance line of <sup>85</sup>Rb. A schematic drawing of the setup is shown in Fig. 1. A tunable external cavity diode laser is used. The laser frequency is actively stabilized and can be locked to an arbitrary point on the resonant line using the dichroic atomic vapor laser lock technique [12]. The laser linewidth as measured with a Fabry-Perot spectrum analyzer is  $\leq 7$  MHz. NMOE signals are detected with a conventional spectropolarimeter. The polarimeter incorporates a crossed Glan prism polarizer and a polarizing beam splitter used as an analyzer. A

Faraday glass element modulates the direction of the linear polarization of the light at a frequency  $\omega_m \approx 2\pi \times 1$  kHz with an amplitude  $\alpha_m \approx 5 \times 10^{-3}$  rad. The first harmonic of the signal from the photodiode PD1, placed in the darker channel of the analyzer, is detected with a lock-in amplifier. It is proportional to the angle of the optical rotation caused by the atoms in the cell,  $\varphi_s$  (see, e.g., [13], and references therein). This signal, normalized to the transmitted light power detected in the brighter channel of the analyzer with a photodiode PD2, is a measure of the optical rotation in the vapor cell. The cell was placed inside a four-layer magnetic shield and surrounded with three mutually perpendicular magnetic coils. The shield was manufactured from 0.040 in. thick CONETIC-AA sheets. The three outer layers of the shield are cylinders with conical lids, while the innermost layer is a cube (12 in. side) with rounded edges. The nearly spherical shape of the three outer layers provides an almost isotropic shielding of the external dc fields by a factor of  $\sim 10^6$ . The layers are spaced with polyurethane foam to reduce mechanical stress. All CONETIC parts were annealed in a hydrogen atmosphere. Although no degaussing was used, the residual magnetic fields averaged over the volume of the vapor cell were found to be at a level of several  $\mu$ G (before compensation).

A NMOE spectrum and a corresponding fluorescence spectrum are shown in Fig. 2. The spectra were taken with  $B_z \approx 40$  mG. At this field in the present geometry, NMOE is primarily due to the transit effect [2,13]. The fluorescence profile of the <sup>85</sup>Rb  $D_2$  line consists of two groups of transitions from the two ground state hyperfine sublevels (total angular momentum  $F_g = 2, 3$ ) to the unresolved hyperfine levels of the excited-state (total angular momentum  $F_e = 1, 2, 3, 4$ ). The transition groups  $F_g = 2 \rightarrow F_e = 1, 2, 3$  and  $F_g = 3 \rightarrow F_e = 2, 3, 4$  are referred to as  $F_g = 2$  and  $F_g = 3$  components of the  $D_2$  line. The dispersively shaped NMOE spectrum for the  $F_g = 3$  component is due to the closed nature of the  $F_g = 3 \rightarrow F_e = 4$  transition [13].

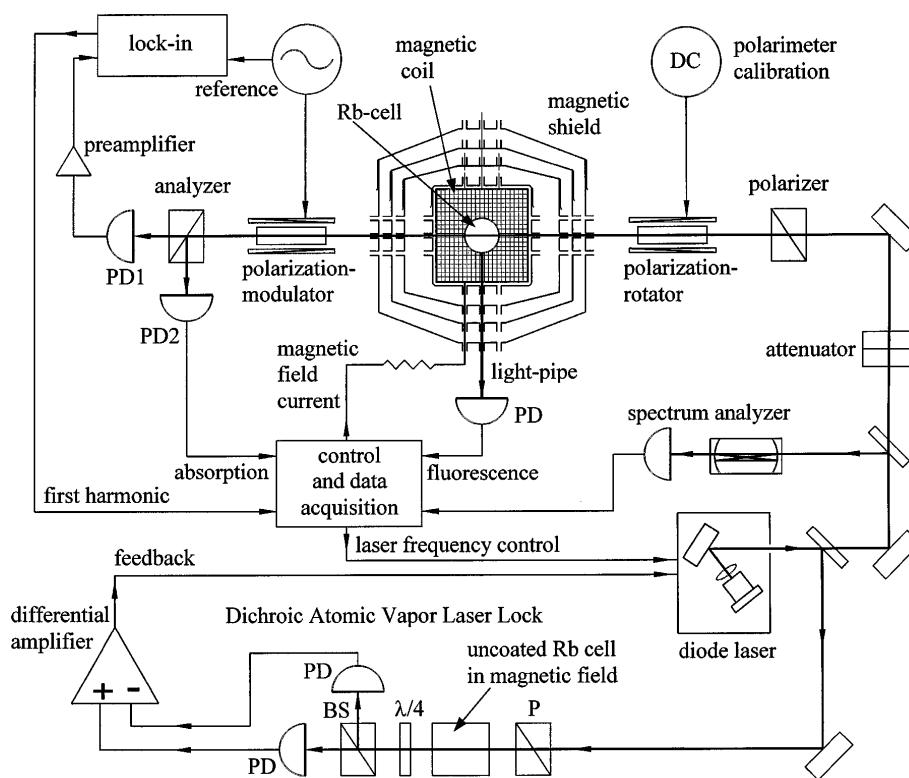


FIG. 1. Schematic diagram of the experimental arrangement.

For this transition, optical pumping leads to increased absorption, rather than bleaching [14] (see below).

In the following we describe experimental results for the  $F_g = 3$  hyperfine component. The optical thickness of the vapor at a temperature of 20.5 °C was measured to be  $d/l_0 \approx 1.4$  for the center of the absorption line. Here  $l_0$  is the unsaturated absorption length. Figure 3 shows the magnetic field dependence of the optical rotation for the laser tuned near the positive peak of the NMOE resonance line for the  $F_g = 3$  component [see Fig. 2(a)]. The overall slope in Fig. 3 is due to the hole-burning effect. The dispersionlike structure is due to the light-induced atomic alignment. Its width  $\Delta B_z \approx 120$  mG is determined by the time of atoms' transit through the laser beam (effective diameter  $\sim 2$  mm). The inset in Fig. 3 shows the near-zero  $B_z$ -field behavior at a  $2 \times 10^5$  magnification. The remarkably narrow feature corresponds to alignment preservation over thousands of wall collisions.

We performed measurements to identify the dominant relaxation mechanisms limiting the smallest width of the NMOE feature. Figure 4 shows the dependences of the effective width on the light intensity at two cell temperatures. These temperatures correspond to Rb vapor densities that differ by about a factor of 2. The light broadening effect is clearly seen in Fig. 4. It arises when atoms aligned in an interaction with the light beam have a high probability of repeated interactions with the light before the alignment is lost due to the light-independent relaxation. These interactions "reset" the alignment. The observed linearity of power broadening at low light intensity

can be explained by this mechanism. Figure 4 also shows three data points taken with the laser frequency tuned to the slope of the resonance line. The laser intensity

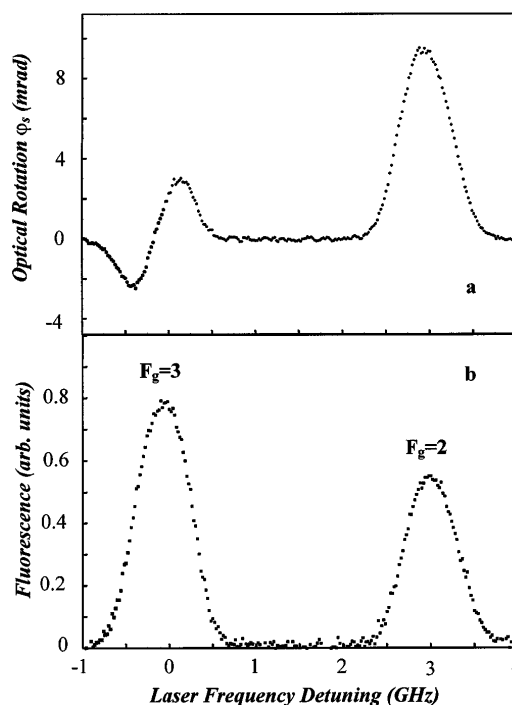


FIG. 2. (a) Experimental NMOE spectrum; (b) the corresponding fluorescence spectrum. Light intensity:  $100 \mu\text{W}/\text{cm}^2$ ;  $B_z \approx 40$  mG.

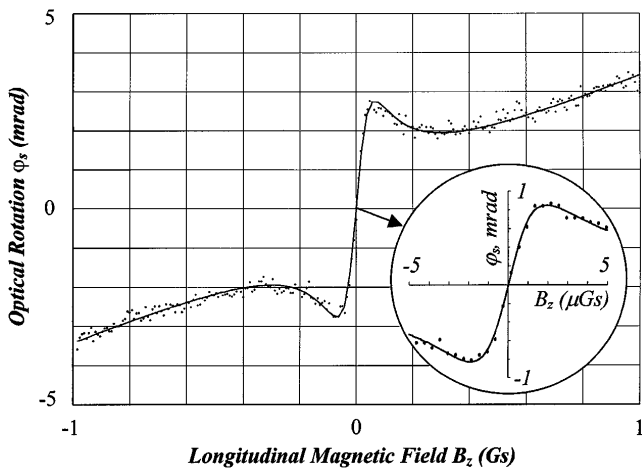


FIG. 3. Optical rotation dependence on the longitudinal magnetic field. Light intensity:  $\approx 100 \mu\text{W}/\text{cm}^2$ ; the laser is tuned to the peak of the  $F = 3$  component of NMOE, corresponding to a  $\approx 150$  MHz high frequency detuning from the peak of the fluorescence (Fig. 2). The solid line is a fit to the model described in the text. The inset shows a detailed scan of the near-zero  $B_z$ -field region.

for these scans was comparable to the highest intensities for the scans at the line center, while the effective relaxation rate was close to the ultimately small rate for that temperature. This can be explained as follows. The repeated interactions of the aligned atoms with light occur only when the atoms return into the laser beam and are in the velocity group resonant with the light. The probability for a given atom to be in a velocity group corresponding to the line wing is smaller than that for the center. Thus, the average time between repeated interactions with light

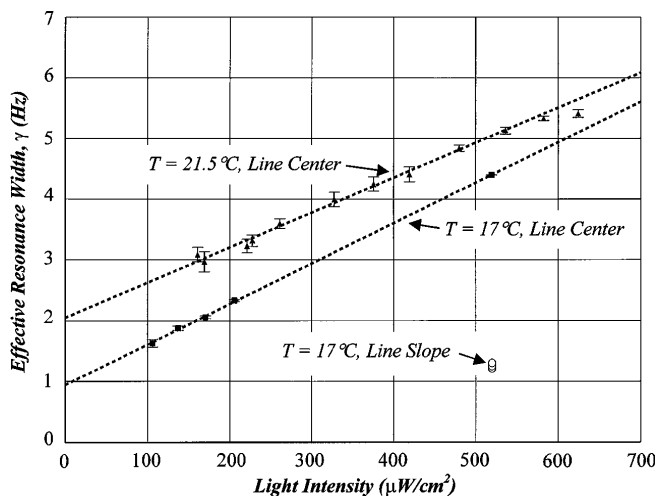


FIG. 4. Effective resonance width dependence on light intensity at two cell temperatures. The values of  $\gamma$  were obtained from the fits to experimental  $B_z$  dependences of NMOE. In the studied light intensity range the magnitude of rotation is approximately proportional to the intensity. The line-slope data were taken on the high frequency slope of the resonance at detunings  $\approx 430$ ,  $\approx 460$ , and  $\approx 485$  MHz (upper, middle, and lower point).

is longer at the wing, making this broadening mechanism less important. This allows one to keep laser intensity relatively high, while avoiding excessive light broadening.

In the zero-power limit, the widths tend to the values, which closely follow the Rb vapor density. We conclude that the spin-exchange collisions are currently the principal relaxation mechanism. The corresponding alignment relaxation cross section is estimated to be  $\sim 10^{14} \text{ cm}^2$ , close to the cross sections of other spin-exchange processes in Rb [11].

The data discussed above were taken with transverse magnetic fields compensated to a level corresponding to a small fraction of the observed widths  $\Delta B_z$ . The presence of transverse magnetic fields  $B_{tr} = (B_x, B_y) \sim \Delta B_z$  dramatically changes the shape of the observed curves [9,15]. Figure 5 shows a series of  $B_z$ -field scans at different transverse magnetic fields. For these scans, the laser was tuned  $\approx 460$  MHz towards high frequencies from the center of the resonance line. The light intensity was  $520 \mu\text{W}/\text{cm}^2$ . The left column in Fig. 5 represents curve shapes with different values of  $B_y$  at a constant  $B_x \approx 2 \mu\text{G}$ . The position of the additional “twist” along the slope of the main feature changes with  $B_y$ , crossing the center at  $B_y \approx 0$ . The right column illustrates the shape dependence on  $B_x$  at  $B_y \approx 0$ . The twist disappears, and the NMOE feature becomes narrower with decreasing the absolute value of  $B_x$ . The central twist is most pronounced when the laser is tuned to the high frequency wing of the  $F_g = 3$  component. In this case the contribution of the closed  $F_g = 3 \rightarrow F_e = 4$  transition to the NMOE signal

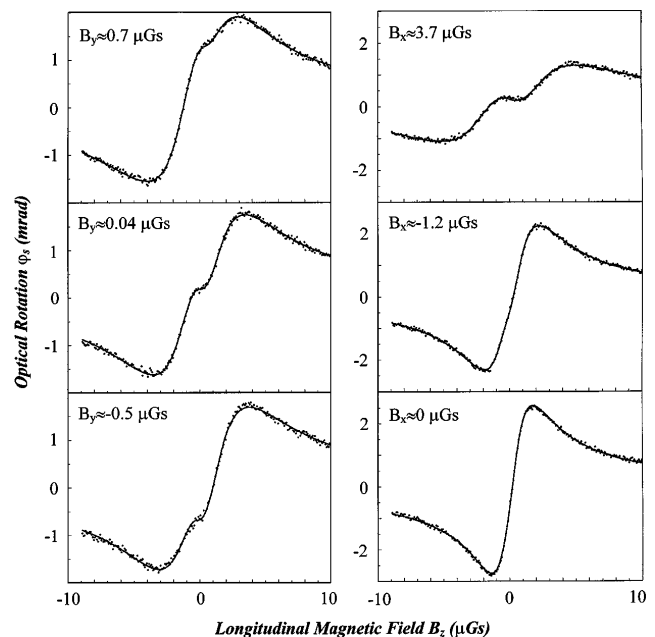


FIG. 5. NMOE dependences on the longitudinal magnetic field with various transverse magnetic fields. The values of  $B_x$  and  $B_y$  are obtained by fitting experimental data with the two-polarizer model (solid lines) described in the text. The linear light polarization incident on the atoms is along the  $x$  direction.

gives rise to an effective alignment perpendicular to the light polarization. Zeroing of transverse magnetic fields is accomplished by finding such currents in the magnetic coils, for which the observed  $B_z$  dependence of NMOE has a symmetric dispersive shape with minimal width. When residual transverse magnetic fields are zeroed (Fig. 5, lower right trace), the effective relaxation width is the narrowest:  $\gamma = g\mu\Delta B_z \approx 2\pi \times 1.3$  Hz (relaxation time  $\tau \approx 250$  ms), where  $g = 1/3$  for the  $F_g = 3$  state.

The NMOE line shapes can be described quantitatively with an intuitive model developed in [6,13], if one extends it to the case of an arbitrarily directed magnetic field [9]. (A more formal approach [16] can also be applied.) In this model, the optical rotation originates from a three-step process: (1) creation of alignment by the incident linearly polarized light. The direction of the alignment is either along or perpendicular to the light polarization depending on whether there is bleaching or an increase in the absorption determined by the nature of the transition; (2) free Larmor precession of the alignment in the magnetic field; (3) modification of the light polarization upon propagation through the medium with rotated alignment. The atomic medium in this case is analogous to a linear dichroic polarizer rotating with the Larmor frequency. In order to describe the line shapes shown in Fig. 5, it is essential that the model includes two independent atomic subsamples with alignments corresponding to polarizers with transmission axes directed mutually perpendicularly. These subsamples arise due to optical pumping through different hyperfine transitions. In the case of  $B_{tr} = 0$ , the NMOE dependences on  $B_z$  for both of these subsamples have symmetrical dispersive shapes of the same widths, but of different signs and magnitudes. Thus, the resulting sum curve has a symmetrical shape without the additional twist. If  $B_{tr} \neq 0$ , the features of the two alignments acquire different asymmetrical shapes leading to the resulting curves shown in Fig. 5.

In conclusion, we have observed ultranarrow features in NMOE with  $\gamma \approx 2\pi \times 1.3$  Hz limited by alignment relaxation in spin-exchange collisions. The improvement in the width from previous results [8,9] is due to elimination of several sources of broadening. First, the use of an atomic cell with a high quality antirelaxation coating made the relaxation from wall collisions negligible compared to the spin-exchange relaxation. Second, accurate control over magnetic field conditions at the vapor cell was achieved by employing a multilayer magnetic shield and by additionally compensating residual fields using the developed NMOE technique itself for sensitive 3-axis magnetometry. Finally, the effect of light broadening was considerably reduced (without attenuating the light power) by working on the slope of the resonance line. The ultranarrow NMOE features were found to have strong non-trivial dependence on transverse magnetic fields, which

is well described by the developed model. The enhancement of the nonlinear optical rotation at near-zero  $B$  fields demonstrated in this work may be used in high-sensitivity low-field 3-axis magnetometry [15]. Another application is searching for parity and time reversal invariance violation in atoms [7,15,17,18]. Similar techniques may also be applied in related research on electromagnetically induced transparency [19], coherent dark resonances [20], phaseonium [21], etc., in order to obtain long coherence times and narrow resonances.

The authors are grateful to E. B. Alexandrov for helpful discussions and for providing the coated cell, and to A. Vaynberg, S. Bonilla, M. Solarz, and G. Weber for manufacturing parts of the apparatus. This research is supported by ONR, Grant No. N00014-97-1-0214.

- 
- [1] W. Gawlik, in *Modern Nonlinear Optics*, edited by M. Evans and S. Kielich, Advances in Chemical Physics Series Vol. LXXXV, Pt. 3 (Wiley, New York, 1994).
  - [2] L. M. Barkov, D. Melik-Pashayev, and M. Zolotarev, *Opt. Commun.* **70**, 467 (1989).
  - [3] M. G. Kozlov, *Opt. Spectrosc. (USSR)* **67**, 789 (1989).
  - [4] V. S. Smirnov, A. M. Tumaikin, and V. I. Yudin, *Sov. Phys. JETP* **69**, 1613 (1989).
  - [5] K. P. Zetie *et al.*, *Opt. Commun.* **91**, 210 (1992).
  - [6] A. Weis, J. Wurster, and S. I. Kanorsky, *J. Opt. Soc. Am B* **10**, 716 (1993).
  - [7] B. Schuh *et al.*, *Opt. Commun.* **100**, 451 (1993).
  - [8] S. I. Kanorsky, A. Weis, and J. Skalla, *Appl. Phys. B* **60**, S165 (1995).
  - [9] D. Budker, V. Yashchuk, and M. Zolotarev, Report No. LBNL-41149, 1997 (to be published).
  - [10] E. B. Alexandrov *et al.*, *Laser Phys.* **6**, 244 (1996).
  - [11] M. A. Bouchiat and J. Brossel, *Phys. Rev.* **147**, 41 (1966).
  - [12] K. L. Corwin, Z.-T. Lu, and C. E. Wieman, *Appl. Opt.* **37**, 3295 (1998).
  - [13] S. I. Kanorsky *et al.*, *Phys. Rev. A* **47**, 1220 (1993).
  - [14] A. P. Kazantsev *et al.*, *Opt. Spectrosc. (USSR)* **57**, 116 (1984).
  - [15] D. Budker, V. Yashchuk, and M. Zolotarev, in *Proceedings of ICAP XVI, Windsor, Canada, 1998, Abstracts* (University of Windsor, Windsor, 1998); Report No. LBNL-42228, 1997 (to be published).
  - [16] G. Nienhuis and F. Schuller, *Opt. Commun.* **151**, 40 (1998).
  - [17] L. M. Barkov, M. S. Zolotarev, and D. Melik-Pashayev, *Sov. JETP Pis'ma* **48**, 144 (1988).
  - [18] L. R. Hunter, *Science* **252**, 73 (1991).
  - [19] S. E. Harris, *Phys. Today* **50**, No. 7, 36 (1997).
  - [20] E. Arimondo, in *Progress in Optics*, edited by E. Wolf (Elsevier, Amsterdam, 1996), Vol. 35, p. 257; S. Brandt *et al.*, *Phys. Rev. A* **56**, R1063 (1997).
  - [21] M. Fleishhauer and M. O. Scully, *Phys. Rev. A* **49**, 1973 (1994).